Energy Efficient Dynamic Optical Routing for Mobile Metro-Core Networks Under Tidal Traffic Patterns

Rodolfo Alvizu, Xingyu Zhao, Guido Maier, Yajing Xu, and Achille Pattavina

***Abstract*—In general, humans follow highly predictable daily movements. We commute from residential to working and/or educational areas in a daily basis, and we have a selection of commercial and recreational areas for the nights and weekends. We also use the mobile phone at regular hours, for example when commuting, during lunch break and at night. Such regular behavior creates predictable spatio-temporal fluctuations of traffic patterns, which in analogy to the periodical rise and fall of the sea levels, its known as tidal traffic phenomenon. In this paper, we propose a suite of on-line matheuristics to reduce energy consumption of optical layer in mobile metro-core networks, while providing $1 + 1$ protection of the aggregated traffic. The proposed matheuristic dynamically optimizes resource allocation by effectively adapting to predictable tidal traffic variations. The optimality of on-line decisions is achieved by generating optimal weighted graphs from the interaction with an off-line optimization phase. In the off-line phase either a wavelength path (WP) or a virtual-WP problem is solved using the regular tidal traffic patterns. Our results display energy savings of more than 20% by introducing load adaptive network operation, while the matheuristic closely follows the optimal results. We also introduce a heuristic method to reduce service disruption due to routing changes, while preserving energy saving capability. The heuristic allows us to reduce service disruption in the range of 38–80% with a small penalty on energy saving of less than 5%.**

***Index Terms*—Dynamic optical routing, energy efficiency, human mobility patterns, mobile network, tidal traffic.**

I. INTRODUCTION

TODAY, the volume of mobile data traffic (cellular) is by far smaller in comparison with its fixed counterpart, but it is growing two times faster. With an expected 10-fold growth from 2016 to 2021 [1], by 2020 mobile data traffic will represent 15% of global IP traffic [2]. The popularity of smartphones, the evolution of 4G and the advent of 5G systems, HD-resolutions mobile-terminal screens, mobile cloud service and the Internet of things are major contributions to the expected mobile data traffic. Since the beginning of 2016 commercial 4G devices support downlink data speeds of 1 Gbps [1], and among the requirements of 5G it is expected a 1000-fold growth of mobile access bandwidth per unit area from 2015 to 2020 [3].

Mobile data traffic refers to data traffic over cellular networks such as 2G, 3G and 4G radio systems. It is important to notice that today, mobile data traffic does not include the traffic from wireless systems such as Wi-Fi, which provides a "wireless" access to a fixed Internet connectivity based, for instance, on xDSL (Digital Subscriber Line technologies), coaxial cable, fiber or even optical wireless access. However, 5G will be the first mobile technology that takes into account the convergence with fixed wireless (fixed and mobile convergence).

Mobile data traffic is very dynamic; nevertheless due to the highly predictable daily movements of large populations of citizens in urban areas [4], the mobile traffic exhibits repetitive patterns with spatio-temporal variations. This behavior has been recently compared to the rise and fall of the sea levels, known as tides. Thus, it was called the tidal traffic scenario [5].

Tidal traffic may create hot spots in the network that move in the spatio-temporal space, following a regular pattern given by the human commutation from residential areas to working areas (academic, business, industrial, medical, governmental among others). Special events may change the tidal traffic, as for instance maintenance, disasters, and social events.

The recognition of regular components in aggregated traffic allowed us to propose in a previous work [6] two off-line optimization methods for dynamic routing and resource allocation of the mobile metro-core network to reduce the energy consumption of the optical layer. Extending our previous work, we now present an on-line matheuristic that reuses the off-line results of regular tidal traffic patterns to improve optimality of on-line decisions upon unexpected traffic variations. Our results show that energy savings of up to 47.5% can be achieved when comparing to a network statically dimensioned for the traffic demand peak.

This is an extension of the work presented in [6], where we proposed two off-line optimization methods to target predictable traffic in urban areas. This models are described in Section IV, and they use dynamic optical resource allocation to minimize energy consumption while providing 1 + 1 protection.

The main contribution of this study is an on-line optimization matheuristic (Algorithm 2) for dynamic optical routing in mobile metro-core networks, able to cope with predictable tidal traffic patterns with unpredictable fluctuations. The matheuristic is based on two phases: 1) *Off-line phase*: exploits tidal traffic phenomenon to solve an optimization problem based on predictable traffic patterns. 2) *On-line phase*: reduces the

This work was supported by the EU FP7 IRSES MobileCloud Project under Grant 612212.

R. Alvizu is with the Dipartimento di Elettronica, Informazione e Bioingegneria, Politecnico di Milano, Milan 20133, Italy, and also with the Department of Electronics and Circuits, Simon Bolivar University, Caracas 89000, Venezuela (e-mail: rodolfoenrique.alvizu@polimi.it).

X. Zhao, G. Maier, and A. Pattavina are with the Dipartimento di Elettronica, Informazione e Bioingegneria, Politecnico di Milano, Milan 20133, Italy (e-mail: xingyu.zhao@mail.polimi.it; guido.maier@polimi.it; achille.pattavina@polimi.it).

Y. Xu is with the School of Telecommunication Engineering, Beijing University of Posts and Telecommunications, Beijing 100876, China (e-mail: xyj@bupt.edu.cn).

Manuscript received August 23, 2016;
revised November 19, 2016 and De-cember 8, 2016;
accepted December 9, 2016.
Date of publication December 11, 2016;
date of current version January 9, 2017.

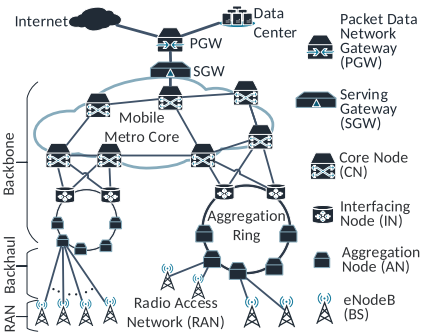

Fig. 1. Reference mobile carrier network (MCN) architecture.

optimality gap of dynamic resource allocation by solving a simple link-disjoint path-pairs algorithm over an optimal weighted graph that is calculated with the off-line phase results.

We have also proposed a scheduling heuristic that provides a good trade-off between reduction of routing changes (to avoid disruption) and resource allocation efficiency (to increase energy savings), applicable to the on-line optimization matheuristic.

The paper is organized as follows: Section II presents related works. In Section III we define the MCN, a procedure to synthesize MCN topology, and a brief analysis of aggregated tidal traffic. The proposed off-line and on-line methodologies are described in Sections IV and V, respectively. The power consumption models and the numerical results are reported in Section VI. Finally conclusions and future works are presented in Section VII.

II. Related works

The mobile carrier network (MCN) traffic has been used to analyze the movements of human beings. In [4], a human mobility analysis from a MCN shows that there is a high predictability (from 80% to 93%) on the user mobility due to the inherent regularity of human behavior.

A study from a Wi-Fi network[1] [7], showed that human mobility is strongly related with time-dependent traffic fluctuations of the network, however they neglected the spatial variations. In this work we consider the influence of spatio-temporal variations of aggregated traffic at the mobile metro-core network (see Fig. 1). The predictability of such three dimensional surface provides valuable information for optimization of dynamic resource allocations.

The energy efficiency limits of networks that can adapt to traffic load variations in time were analyzed in [8]. However, given that base stations are the most power-hungry devices in MCN architectures, dynamic resource allocation and energy efficiency efforts in MCN are mainly focused on the RAN (see Fig. 1) [9], [10]. Most of the works on resource allocation and energy efficiency optimization take into account only the temporal fluctuation of an overall traffic demand. However, such homogeneous traffic matrix is far from the behavior of traffic load in a metropolitan area.

The combined effect of temporal and spatial variations of traffic was first proposed for energy efficient operation of access networks. Tidal traffic was first considered for optimization of RANs, considering a small cluster of MCN cell sites [5]. Then, in [11] tidal traffic was used to proposed energy efficient management for passive optical networks.

Recently, tidal traffic effect was considered in [12], [13] to propose energy efficiency in metropolitan networks. A limitation of these works, is that they assumed mainly two basic tidal traffic patterns: residential and business. However, the social composition of metropolitan areas is more complex than just residential and business, and multiple social functions or services can coexist in the same location. In this work we consider the MCN traffic from several different locations in the urban area, thus we are able to capture different types of traffic patterns.

[1] Wi-Fi network traffic is not considered as mobile data traffic.

III. The mobile carrier network and the tidal traffic patterns

In this work we propose a suit of methodologies that exploit the presence of regular aggregated-traffic patterns in the MCN and employ short-term traffic predictions to improve the use of dynamic optical resource allocation. However, traffic pattern recognition, and traffic demand prediction techniques are not the focus of this work. Our main focus is the optimization of dynamic resource allocation techniques to minimize the energy consumption of optical metro-core networks.

We have used a MCN real dataset that contains anonymized detailed call records of 4869 cells from a mid-sized city of China, over a two-month time period, and real cell site geographical locations. This section starts defining the general MCN architecture. Then, it describes a procedure to synthesize the MCN network architecture. Finally, it provides a brief description and an example of the aggregated tidal traffic patterns that we have used.

A. MCN Architecture

In this paper we based our assumptions on LTE current deployment, but the same architecture remains valid also to support a future evolution to 5G. As depicted in Fig. 1, the MCN is commonly modeled with a three-level hierarchical architecture, composed by the radio access, the *back-haul* and the *backbone* networks [14], [15]. The *base stations* (BS)s deployed on the field provide radio access. Each BS (comprising a set of cell antennas and an eNodeB) is connected by a back-haul network segment to an *aggregation node* (AN). The ANs are the edge elements interfacing the back-haul to the backbone network. The backbone network is the infrastructure connecting the ANs to the *serving gateway* (SGW). We assumed that the metro backbone is divided into an aggregation and a core segment, in order to gradually groom traffic of the metro area from the edges towards the SGW. The *aggregation network* is composed by metro optical rings, each one connecting a subset of neighbor ANs. On every ring, two ring nodes, called *interfacing nodes* (IN)s, are used to interface the aggregation to the core segment of the backbone network. Each IN is connected to a *core node* (CN) of the core network (Fig. 1). The *mobile metro-core network* is the mesh-topology fiber infrastructure interconnecting the core nodes and the SGW. The assumption of mesh topology of the core is consistent with the current evolutionary trend leading from ring to mesh in the metro areas, given the abundance of fiber links in large cities. We suppose that each node of the core network is an optical cross connect (OXC).

The SGW is connected to a *packet gateway* (PGW) which provides connectivity towards data center facilities and Internet Exchange Points (IXP)s. It is important to notice that all the

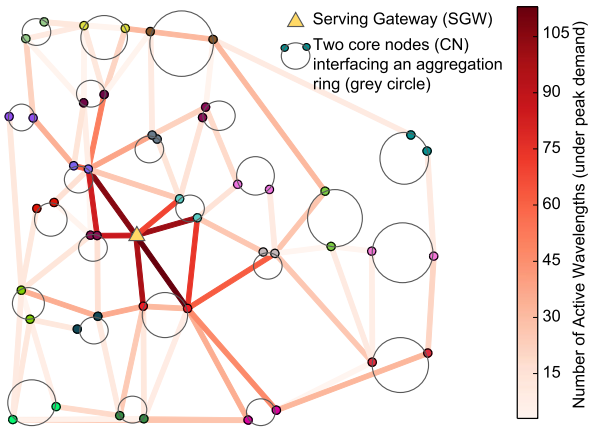

Fig. 2. Synthetic topology of the Chinese city based on real location data and a conservative dimensioning on the peak.

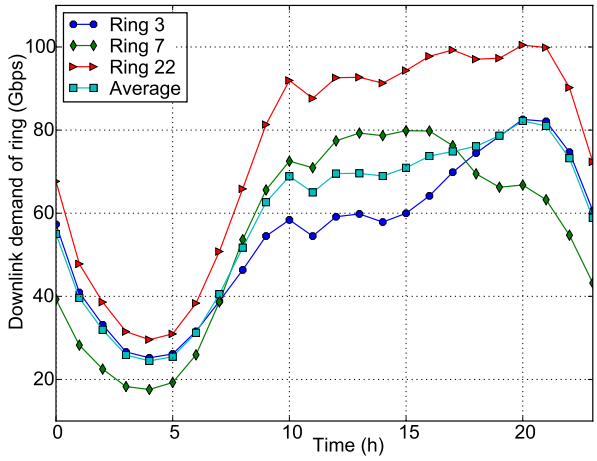

Fig. 3. Predictable aggregated tidal traffic demands (down-link) $H_{j,t}^{DL}$.

mobile data traffic must pass through the metro SGW: therefore the part of network which extends from the SGW to the PWG and beyond has not been included in this study.

Given that the connections in the MCN transports large volumes of traffic to/from aggregation rings, and should meet service level agreements to offer carrier grade services, we assumed that these connections need to be provisioned with 1 + 1 protection scheme [16]. The combination of aggregation rings and mesh core, together with the dual-homed interconnection of each ring to the core, enables full resilience of the physical infrastructure of the entire mobile metro backbone against (at least single) failures. The methodologies proposed in the following sections introduce 1 + 1 protection with a pair of edge disjoint paths obtained with Algorithm 1, which establishes the active and backup path on different INs of each ring. Offering 1 + 1 protection is still simple, because it can be seen as the establishment of two link-disjoint dedicated connections for each request instead of a single path. Moreover, we avoided the shared path protection scheme to keep the problem simpler [17].

The MCN topology was synthesized from the real geographical location of 4869 BSs of an anonymous Chinese city: 1) *RAN:* starting from the BSs, we used a clustering algorithm that creates groups of 10 to 12 BSs by minimizing the distance between BSs and the AN of the cluster. 2) *Aggregation rings:* from the set of ANs, a second level of clustering was performed to create 23 aggregation rings of 20 ANs each. 3) *Metro-core:* from each ring two nodes where marked as the INs. The metro-core is composed by 46 CNs and one SGW, connected by multi-fiber links (with 80 wavelengths per fiber) in a maximal planar graph with degree 6. Finally, we set the number of fibers of each link of the metro-core network to minimize CapEx, assuming every ring is generating traffic at the daily peak. This dimensioning was done by solving two multi-commodity problems using VWP and WP (for simplifying the presentation, we do not describe these formulations, while VWP and VP are introduced in Section IV). The resulting network for WP model is shown in Fig. 2.[2]

B. Regular tidal traffic patterns

We have used a MCN real dataset that does not provide the mobile data traffic information. In consequence, in our previous work [6] we presented a methodology to estimate regular tidal traffic patterns considering: 1) the average number of mobile users $N_{c,t}$ in each cell c, at each hour t over the two month dataset, 2) the typical traffic intensity per user at time t, and 3) the capacity of the MCN cells.

Humans in urban areas display regular patterns of behavior with up to 93% of predictability [4]. Therefore, the regular spatio-temporal variation of the number of mobile users $N_{c,t}$, follows tidal fluctuations (regular rise and falls). A substantial correlation has been observed [18], [19] between the profiles of $N_{c,t}$ and the social functions (i.e., residential area, educational zones and commercial districts) which are prevalent in the area covered by the cell. Using the methods proposed in [19] we can analyze the composition of aggregation rings of MCN in terms of social functions.

Fig. 3 depicts an example of the aggregated tidal traffic patterns estimated in [6]. $H_{j,t}^{DL}$ is the total (down-link; DL) bandwidth volume of aggregation ring j at time t. For instance, Ring 7 covers mainly scenic/historic regions that people use to visit during the day: observing the curve in Fig. 3, $H_{7,t}^{DL}$ starts decreasing at $t = 16$, in opposite to the average tendency that starts decreasing at $t = 20$.

IV. Off-line Energy-aware Dynamic Bandwidth Allocation

The role of the mobile core network is to connect CNs to the SGW (see Fig. 1). Therefore, the MCN has to satisfy all up-link (UL) and down-link (DL) demands between aggregation rings and SGW. We assumed all these connections are provisioned with $1 + 1$ protection scheme.

The common practice in MCNs is to perform a static resource allocation to meet the peak-hour demand. This method leads to poor energy efficiency, because the resources will be over-provisioned outside of the peak hour.

An operator can use optimization procedures to dynamically adapt the used resources to the actual hourly need, thus reducing energy consumption. In this section we present two mixed integer linear programming (MILP) formulations to minimize the energy consumption of the MCN (as depicted in Fig. 1) by activating and deactivating resources. By exploiting the predictability of tidal traffic patterns ($H_{j,t}^{UL}$ and $H_{j,t}^{DL}$), these MILP models can be solved off-line.

[2]Aggregation rings are shown just for an illustrative purpose but they are not actually part of the metro-core network.

Algorithm 1: k pairs of link disjoint path: k-PLDP

Given the original graph $\mathcal{G}$, create $\mathcal{G}'$ by introducing a dummy node j $\mathcal{V}' = \mathcal{V} \cup j$, and two directed dummy links $\mathcal{E}' = \mathcal{E} \cup (e^{d1}, e^{d2})$ that connects with the two interfacing nodes v of the aggregation ring j. For DL $src = sgw$, $dst = j$, and e^{d1}, e^{d2} are incoming links of j. For UL $src = j$, $dst = sgw$, and e^{d1}, e^{d2} are outgoing links of j. P and B: sets of working and protection paths, where $b_p \in B$ is link disjoint with working path $p \in P$

1: $P \leftarrow$ k shortest paths between j and sgw (Yen's Algorithm).
2: $B \leftarrow \emptyset$
3: **for** each path $p \in P$ **do**
4: Create a modified weights graph $\mathcal{G}''$ by making cost of links $e \in p$ a big number.
5: $b_p \leftarrow$ Shortest path between j and sgw in $\mathcal{G}''$, to get a possible backup path of p
6: **while** $b_p \in B$ **do**
7: $b_p \leftarrow$ next shortest path (Dijkstra algorithm) between j and sgw in $\mathcal{G}''$, to get another possible backup path of p
8: $B \leftarrow B \cup b_p$
9: **return** (P, B)

In the following subsections we present two formulations for energy-aware dynamic bandwidth allocation problem that differ from each other in the wavelength conversion capability:

1. Virtual Wavelength Path (VWP) model: at each OXC all wavelengths are converted to the electrical domain, allowing to perform wavelength conversion and traffic grooming to increase wavelength utilization. In VWP an optical path can have a different wavelength on each distinct link.

2. Wavelength Path (WP) model: at each OXC wavelengths can either be converted to electrical domain or be switched at the optical domain. WP takes advantage of the small distances[3] in the network to establish fully transparent lightpaths with optical bypass to avoid optical-to-electrical conversions in transit nodes, but also dropping wavelength conversion capabilities. In WP, the same wavelength has to be assigned to an optical path on every link.

VWP and WP are multi-commodity flow problems known to be NP-complete. Therefore, we have use path formulations in order to simplify this problems. In path formulation a set of k candidate path pairs with 1 + 1 protection is pre-calculated for every demand in the network using Algorithm 1. See subSection IV-D for the analysis of complexity of the proposed models and Algorithm 1.

In order to cope with unforeseen traffic increase (e.g., due to flash-crowd events), both formulations reserve 10% of the wavelength channels ($\epsilon = 0.1$) in each active fiber to allow flexibility upon unexpected traffic demand increases; see (1e) and (2e).

A. Problem definition

The optical metro-core network can be represented by a bi-directed graph $\mathcal{G}(\mathcal{V}, \mathcal{E})$, with $V = |\mathcal{V}|$ and $E = |\mathcal{E}|$ nodes (OXCs) and (directed) fiber links, respectively. Let us consider the line rate of the wavelengths $L = 10$ Gbit/s, and the maximum number of channels per fiber $W = 80$. Each demand $d \in \mathcal{D}$ is described by the source and destination pair, and the throughput of such demand $h_{d,t}$ (in Gbit/s) which varies in time t. Each demand $d \in \mathcal{D}$ requests $r_d = \lceil h_d/L \rceil$ wavelength connections which can be split and provisioned with $1 + 1$ protection (two link-disjoint paths per connection $r \in r_d$). A demand $d \in \mathcal{D}$ can be Up-link (UL) from an aggregation ring $j \in \mathcal{J}$ towards the SWG or Down-link (DL) from the SWG to j. As depicted in Fig. 1 each aggregation ring j has two interfacing nodes $v \in \mathcal{V}$.

The off-line planning problem consists in finding the set of paths that satisfies the spatio-temporal -dependent demand matrix of a specific time period t using $1 + 1$ protection, with the objective of minimizing the energy consumption of the optical layer of the mobile metro-core network.

B. Virtual Wavelength Path (VWP)

A path formulation of VWP optimization problem is presented in equation (1).

Parameters: each demand $d \in \mathcal{D}$ requests h_d Gbit/s. Pre-calculated path pairs are given by parameter δ_{edp} ($\delta_{edp} = 1$ if link e belongs to the path pair p realizing demand d, zero otherwise), which is obtained with the Algorithm 1.

Variables: routing assignment for working and protection path pair is given by variables x_{rdp} [1 if r-th connection of demand d is routed on path pair (working and protection) p, zero otherwise]. The integer variables w_e and f_e represent active wavelengths and fibers.

$$\text{Minimize } (\alpha + \mu + \gamma + \zeta) \sum_{e \in \mathcal{E}} f_e + \beta \sum_{e \in \mathcal{E}} w_e \tag{1a}$$

$$\Sigma_{p \in \mathcal{P}_d} x_{rdp} = 1, \quad d \in \mathcal{D},\ r \in \mathcal{R}_d \tag{1b}$$

$$\Sigma_{r \in \mathcal{R}_d} \Sigma_{d \in \mathcal{D}} \Sigma_{p \in \mathcal{P}_d} x_{rdp}\ \delta_{edp} \ \leq \ w_e, \quad e \in \mathcal{E} \tag{1c}$$

$$w_e \leq f_e W, \quad e \in \mathcal{E} \tag{1d}$$

$$f_e \leq (1 - \epsilon) F_e, \quad e \in \mathcal{E} \tag{1e}$$

$$x_{rdp} \text{ binary}, \ \ w_e \in Z^+, \ \ f_e \in Z^+ \tag{1f}$$

Objective: (1a) minimization of number of active fibers f_e and wavelengths w_e that are routing-dependent variables affecting the power consumption.[4]

Constraints: solenoidality constraint (1b) enforces the provision of bandwidth to each connection request. Expression (1c) determines the number of active wavelengths per link, and (1d) imposes an upper bound. Constraint (1e) limits the number of active fibers per link to F_e, and reserves some capacity (ϵ) to cover unexpected traffic demands. F_e is calculated in the static network-dimensioning phase, as presented in Section VI.

C. Wavelength Path (WP)

A path formulation of WP is presented in equation (2).

Parameters: The pre-calculated working and backup paths are given by the parameter δ^w_{edp} ($\delta^w_{edp} = 1$ if link e be-

[3] Regeneration is normally needed after 1500 km for non-coherent wavelength channels at 10 Gbit/s [20].

[4] Symbols $\alpha, \beta, \mu, \gamma, \zeta$, are defined in Section VI-A.

longs to path pair p realizing working path of demand d on any wavelength, zero otherwise), and δ^p_{edp} ($\delta^p_{edp} = 1$ if link e belongs to path pair p realizing protection path of demand d on any wavelength, zero otherwise) obtained with Algorithm 1.

Variables: routing and wavelength assignment (RWA) of working and protection paths are given by binary variables $x_{drp\lambda}$ ($x_{drp\lambda} = 1$ if working path of r-th connection of demand d is routed on path p and wavelength λ, zero otherwise) and $y_{drp\lambda}$ ($y_{drp\lambda} = 1$ if protection path of r-th connection of demand d is routed on path p and wavelength λ, zero otherwise). The number of active wavelengths and fibers per link are represented by variables w_e and f_e, respectively.

$$\text{Minimize} \sum_{e\in\mathcal{E}}(\alpha+\mu+\gamma)f_e \tag{2a}$$

$$\Sigma_{p\in\mathcal{P}_d}\Sigma_{\lambda\in\mathcal{W}}x_{drp\lambda} = 1, \quad d\in\mathcal{D},\ r\in\mathcal{R}_d \tag{2b}$$

$$\Sigma_{\lambda\in\mathcal{W}}x_{drp\lambda} = \Sigma_{\lambda\in\mathcal{W}}y_{drp\lambda}, \quad d\in\mathcal{D},\ r\in\mathcal{R}_d,\ p\in\mathcal{P}_d \tag{2c}$$

$$\Sigma_{d\in\mathcal{D}}\Sigma_{r\in\mathcal{R}_d}\Sigma_{p\in\mathcal{P}_d}(x_{drp\lambda}\delta^w_{edp} + y_{drp\lambda}\delta^p_{edp}) \le f_e, \quad e\in\mathcal{E},\ \lambda\in\mathcal{W} \tag{2d}$$

$$f_e \le (1-\epsilon)F_e, \quad e\in\mathcal{E} \tag{2e}$$

$$\Sigma_{d\in\mathcal{D}}\Sigma_{r\in\mathcal{R}_d}\Sigma_{p\in\mathcal{P}_d}\Sigma_{\lambda\in\mathcal{W}}x_{drp\lambda}\delta^w_{edp} + y_{drp\lambda}\delta^p_{edp} = w_e, \quad e\in\mathcal{E} \tag{2f}$$

$$w_e \le f_e W, \quad e\in\mathcal{E} \tag{2g}$$

$$x_{drp\lambda}\ \text{binary},\ y_{drp\lambda}\ \text{binary},\ f_e\in R^+,\ w_e\in R^+ \tag{2h}$$

Objective: (2a) minimizes the number of active fibers f_e, that is the only routing dependent variable that affects the power consumption at the optical layer of WP (as explained in Section VI-A).

Constraints: (2b) enforces the provision of each connection request. Constraint (2c) forces the utilization of a single path pair p to route the same request. Equations (2d) and (2e) determine and constrain the number of active fibers per link, reserving some capacity (ϵ) to allow unexpected traffic demand meeting the wavelengths continuity constraint. Equation (2f) determines the number of active wavelengths per link, that are constrained to $f_e W$ by (2g).

D. Complexity Analysis

Both WP and VWP are known to be NP-hard problems [16]. To give an idea of their complexity, we evaluated the number of constraints and variables of the proposed formulations (1) and (2). We indicate with R and K the average number of connection requests per each demand and the number of pairs of link disjoint paths, respectively. We can state that the number of constraints of VWP grows as $O(V(V-1)R)$, while for WP grows as $O(V(V-1)R(K+1))$. From the analysis of the variables introduced in the formulations, we can state that the number of variables in VWP grows as $O(V(V-1)RK)$, while WP grows as $O(V(V-1)RKW)$.

In order to simplify the problems, we have used path formulations to constrain the number of possible link disjoint path pairs to a given number (K). Using Yen's algorithm for k-shortest paths, and Dijkstra's algorithm implemented using a Fibonaci heap, the worst case complexity of Algorithm 1 is $O(k^2E(V+ElogE))$.

TABLE I
OPTIMAL LINK WEIGHTS ($c_{e,\hat{r},d,t}$) FOR VWP

Given the $\hat{r}$-th connection request of demand d at time t

Edge e condition	Predicted $\hat{r}_{d,t} \le r_{d,t}$ $c_{e,\hat{r},d,t} =$	Unpredict. $\hat{r}_{d,t} > r_{d,t}$ $c_{e,\hat{r},d,t} =$
Assigned	1	Not possible
Available	$(\omega+1)$	σ
Available-inactive	$(\omega+1)\Delta$	Δ
Unavailable	$\mathcal{M}$	$\mathcal{M}$

$\mathcal{M}$: *big M*, $\sigma << 0$, ω = Length of backup path of $(\hat{r}, d, t)$ tuple
Δ: *fiber-to-wavelength activation cost ratio* ($\Delta > 0$)

V. ON-LINE DYNAMIC BANDWIDTH ALLOCATION

The off-line approach presented in Section IV is based on the regular tidal traffic patterns of the mobile network to propose the use of MILPs to find optimal solutions to RA and RWA problems. However, as solving MILPs is time consuming it cannot be used for on-line decisions (fraction of second) upon unpredicted traffic variations. Heuristics are the common approach for on-line decision making. Algorithm 2 describes a proposed matheuristic for on-line RA or RWA (for VWP and WP respectively). Algorithm 2 is based on two phases:

Phase 1 – Off-line Planning Optimization: based on the MILP models of Sections IV-B and IV-C. Such models are solved for each $t\in\mathcal{T}$ using the predictable (regular) demand matrix ($h_{d,t}$) of an average weekday and weekend.

Phase 2 – On-line Routing: heuristic method that favors optimality by running a minimum cost algorithm on a set of optimally vertex-weighted graphs $\hat{\mathcal{G}}$. The optimal weights calculation is based on the solution $\mathcal{S}_t$ obtained in phase 1.

Initially the set of reconfiguration time points $\mathcal{T}$ is composed by every hour of the day. However, hourly reconfigurations ($|\mathcal{T}| = 24$) is not well accepted by service operators because it leads to service disruption and instability of distributed routing algorithms, such as OSPF and EIGRP. Therefore in subSection V-D we present a simple scheduling heuristic to reduce the reconfiguration time points $|\mathcal{T}| < 24$.

Due to the wavelength assignment of the WP model, a layered graph $\mathcal{G}'$ is needed to perform RWA with a minimum-cost path algorithm. Thus, in subSection V-B1 we present the vertex-weighted layered graph $\hat{\mathcal{G}}'$, and subSection V-C describes the proposed modification of the well-known pair of edge disjoint path algorithm for $\hat{\mathcal{G}}'$.

A. Optimal weights for VWP model

For each $\hat{r}\in\{1..\hat{r}_{d,t}\}$ belonging to demand d at reconfiguration point t, a set of weights $\mathcal{C}_{d,t}$ is generated. Table I summarizes the 8 possible link weights $c_{e,\hat{r},d,t}$ that can be assigned to the vertex-weighted graph $\hat{\mathcal{G}}$. When comparing the regular traffic demand $h_{d,t}$ with the short-term prediction[5] $\hat{h}_{d,t}$, there are two type of requests: *Predictable* ($\hat{r}_{d,t} \le r_{d,t}$): all requests

[5]In this article we do not focus on the short-term prediction methods. Thus we assumed to have a perfect prediction method that basically provides the precise traffic demand of the next reconfiguration time point. We refer the reader to [21] for a comparison on traffic prediction methods.

Algorithm 2: On-line Routing Matheuristic

Solve off-line optimization models using the predictable demand matrix, and generate on-line optimal weights to reduce the routing problem to a Minimum cost algorithm

Phase 1 – Off-line Planning Optimization

Given historical traffic data-set $h_{d,t}$ (large observation windows)

1: **for** $d \in \mathcal{D}$ **do** ▷ *$\mathcal{D}$ Set of demands*
2: **for** $t \in \{1, 2, ..., 23, 24\}$ **do** ▷ *One reconfiguration per hour*
3: **Get** $h_{d,t}$: the regular (predictable) aggregated traffic demand of an average weekday or weekend (Section III-B)
4: **Compute** $\mathcal{T}$: set of reconfiguration time points which can be: Hourly $|\mathcal{T}| = 24$ or Scheduled $|\mathcal{T}| < 24$ (in Section V-D we present a reconfiguration time points scheduling algorithm)
5: **for** $t \in \mathcal{T}$ **do**
6: **Solve** Optimization problem, get optimal solution $\mathcal{S}_t$ using: VWP (Section IV-B) or WP (Section IV-C)

Phase 2 – On-line Routing

7: **for** $t \in \mathcal{T}$ **do** ▷ *One reconfiguration per hour*
8: **for** $d \in \mathcal{D}$ **do** ▷ *$\mathcal{D}$ Set of demands*
9: *Step 2.1 - Short-time traffic prediction*
Given long-term prediction $h_{d,t}$ and the current traffic demand $\bar{h}_{d,t}$, **Predict** $\hat{h}_d$: the short-term traffic demand for the next reconfiguration point.
10: *Step 2.2 - Optimal weights computation*
Given optimal $\mathcal{S}_t$ and the relation between $h_{d,t}$ and $\hat{h}_{d,t}$
Compute $\mathcal{C}$: the weights of the optimal-weighted graph for each connection request $\hat{r}_{d,t} = \lceil \hat{h}_{d,t}/L \rceil$, where L is the line rate (see algorithms in Section V-A and V-B)
11: **for** $\hat{r} \in \{$ Real-time requests belonging to d at $t\}$ **do**
12: *Step 2.3 - Minimum cost algorithm*
Given the optimal-weighted graph of step 2, **Compute** routing using a greedy algorithm based on Bhandari for VWP or on its modification (sec. V-C) for WP.

$\hat{r}$ are optimally planed. *Unpredictable* ($\hat{r}_{d,t} > r_{d,t}$): a sub-set of the requests are optimally planed $\{\hat{r} | \hat{r} \leq r_{d,t}\}$, while another subset is unexpected $\{\hat{r} | \hat{r} > r_{d,t}\}$.

Depending on the off-line optimal planning results, for each request $\hat{r} \in \{1..\hat{r}_{d,t}\}$ there are 4 possible conditions of links $e \in \mathcal{E}$: *Assigned:* e belongs to the $\hat{r}$-th pair of working and backup paths. *Available:* e has at least one free wavelength (not assigned to any request or demand) in active fibers. *Available-inactive:* there is at least one inactive fiber of e. *Unavailable:* e has no free wavelengths.

B. Optimal weights for WP model

In this work we use an equivalent weighted-layered-graph transformation $\hat{\mathcal{G}}'$ in order to reduce the RWA with 1 + 1 protection to finding a pair of edge-disjoint paths in $\hat{\mathcal{G}}'$, at step 2.3 of the matheuristic presented in Algorithm 2. Before describing the optimal weight computation for WP models, we first characterize $\hat{\mathcal{G}}'$ as proposed by Chen *et al.,* in [22].

Algorithm 3: Pair of link disjoint path over layered graph

1: Compute shortest path P_1 in $\hat{\mathcal{G}}'$ using Dijkstra algorithm
2: Set the weight of each virtual arc $a' \in P_1$ and all other virtual arcs related to the same physical path to a large number $c'_a = \mathcal{M}$
3: Negate the cost of the opposite directed arcs of P_1, such modified graph is called $\hat{\mathcal{G}}''$
4: Compute the shortest path P_2 using a modified Dijkstra or a BFS algorithm in $\hat{\mathcal{G}}''$
5: Build a reduced graph $\hat{\mathcal{G}}^{reduced}$ with paths P_1 and P_2, erase the interlacing links between P_1 and P_2
6: Given $\hat{\mathcal{G}}^{reduced}$ use the simple two step approach to get the shortest pair of link disjoint paths

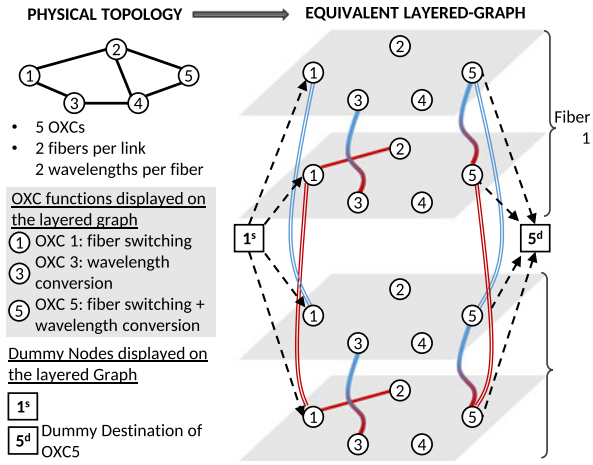

Fig. 4. Equivalent layered-graph $\mathcal{G}'$ for the physical topology shown in the top left corner, and considering only two dummy nodes $1^s \in \mathcal{V}^s$ and $5^d \in \mathcal{V}^d$ where a demand from OXC1 to OXC5 can be mapped.

1) The layered-graph: The equivalent layered-graph transformation allows to perform RWA with a minimum cost algorithm (step 3 of the on-line routing for WP). Given the graph $\mathcal{G}(\mathcal{V}, \mathcal{E})$ (defined in Section IV), it can be represented by its equivalent layered-graph $\mathcal{G}'(\mathcal{V}', \mathcal{E}', \mathcal{V}^s, \mathcal{A}^s, \mathcal{V}^d, \mathcal{A}^d)$. In $\mathcal{G}'$, each node $\mathcal{V}$ and link $\mathcal{E}$ in the original graph $\mathcal{G}$ is replicated WF times as virtual nodes $\mathcal{V}'$ and virtual links $\mathcal{E}'$. The virtual nodes of node $v \in \mathcal{V}$ are denoted as $v^{\lambda f}$, with wavelengths $\lambda \in \{1..W\}$ and fibers $f \in \{1..F\}$. The virtual links of link $e \in \mathcal{E}$ are denoted as $e^{\lambda f}$, with $\lambda \in \{1..W\}$ and $f \in \{1..F\}$. For each node $v \in \mathcal{V}$ in the original graph two extra dummy nodes are added, where source and destination of the demands $\mathcal{D}$ are mapped. The dummy source node related to node v, denoted as $v^s \in \mathcal{V}^s$, only has outgoing dummy-arcs $\mathcal{A}^s$ towards the virtual replicas of node v ($v^{\lambda f}$). The dummy destination node $v^d \in \mathcal{V}^d$, only has incoming dummy-arcs $\mathcal{A}^d$ from the virtual replicas of node v ($v^{\lambda f}$).

Fig. 4 depicts an example of $\mathcal{G}'$ for a 5 nodes network (top left of the figure), with $F = 2$ fibers per link and $W = 2$ wavelengths per fiber. In the example, wavelength conversion is possible at nodes 3 and 5, while fiber switching is enabled at nodes 1 and 5. To simplify the presentation of Fig. 4, only two dummy nodes with its corresponding 4 directed dummy-arcs are depicted, even if there are in total 10 dummy nodes and 20 outgoing and 20 incoming dummy-arcs in this network.

Algorithm 4: Reconfiguration time point Scheduling $(\bar{\eta}, H)$.

1: $\bar{T} \leftarrow 0$ $\quad \triangleright \bar{T}$: maximum number of reconfigurations
2: **while** $\eta < \bar{\eta}$ **do** $\quad \triangleright \bar{\eta}$: expected efficiency, see equation (3)
3: $\quad \bar{T} \leftarrow \bar{T} + 1$ $\quad \triangleright \mathcal{T}$: set of reconfiguration time points
4: $\quad$ **do** *Simulated Annealing* to Find reconfiguration schedule $\mathcal{T}$ such that $|\mathcal{T}| == \bar{T}$ and with maximum efficiency η
return $\mathcal{T}$, the reconfiguration scheduling with min. number of reconfiguration time points and expected allocation efficiency

TABLE II
OPTIMAL VIRTUAL LINK WEIGHTS ($c_{e',\hat{r},d}$) FOR WP

Given the $\hat{r}$-th connection request of demand d at time t

Virtual Link e' condition	Predicted $\hat{r}_{d,t} \leq r_{d,t}$ $c_{e',\hat{r},d,t} =$	Unpredict. $\hat{r}_{d,t} > r_{d,t}$ $c_{e',\hat{r},d,t} =$
Working	σ	Not possible
Backup	1	Not possible
Available	$(\omega + 1)$	σ
Inactive	$(\omega + 1)\Delta$	Δ
Unavailable	$\mathcal{M}$	$\mathcal{M}$

$\mathcal{M}$: *big M*, $\quad \sigma << 0$, $\quad \omega =$ Length of backup path of $(\hat{r}, d, t, i)$ tuple
Δ: *fiber-to-wavelength activation cost ratio* $(\Delta > 0)$

2) Optimal Weights for WP in the layered graph: For each $\hat{r} \in \{1..\hat{r}_{d,t}\}$ belonging to demand d at the next reconfiguration point t, a set of weights $\mathcal{C}'_{d,t}$ is generated. Table II summarizes the 10 possible weights $c'_{e',\hat{r},d}$ that can be assigned to the virtual links ($e^{\lambda f}$ will be called e' for simplicity) of the vertex-weighted layered-graph $\hat{\mathcal{G}}'$. As described in Section V-A, there are two type of requests: predictable and unpredictable demands. Depending on the off-line optimal planning results S_t (phase 1 of Algorithm 2), there are 5 possible conditions of links $e' \in \mathcal{E}'$: *Working:* e' belongs to the $\hat{r}$-th working path of d. *Backup:* e' belongs to the $\hat{r}$-th backup path of demand d. *Available:* e' is a free wavelength of an active fiber. *Inactive:* e' belongs to an inactive fiber of e. *Unavailable:* e' is assigned to other requests $(r'|r' \neq \hat{r})$, or to other demands $(d'|d' \neq d)$.

In the layered graph $\hat{\mathcal{G}}'$, the cost of dummy arcs is always equal to zero $c_a = 0$.

C. Link-disjoint path-pairs computation

After computation of weights, an algorithm is used to compute the pair of link-disjoint paths to assign to protected request $\hat{r} \in \{1..\hat{r}_{d,t}\}$ belonging to demand $d \in \mathcal{D}$ at time t.

Each link $e \in \mathcal{E}$ belonging to the original graph $\mathcal{G}$ is replicated WF times as virtual links $e' \in \mathcal{E}'$ in the layered graph $\mathcal{G}'$. Therefore, virtual-edge disjointness on $\mathcal{G}'$ do not guarantee physical edge disjointness on $\mathcal{G}$. Thus, we have implemented a minimum cost greedy algorithm based on Bhandari's link-disjoint path algorithm [23]. Algorithm 3 describes the implemented extension of Bhandari's algorithm to enforce physical edge disjointness in a weighted layered graph (here after called modified Bhandari algorithm).

TABLE III
ENERGY DISSIPATION AND DISRUPTION RATE TRADE-OFF

	VWP		WP	
	Hourly	Scheduled	Hourly	Scheduled
Total Energy (kWh)	1760	1850.6	1314	1358.3
Energy Saving (compared to static)	29.7%	26.1%	23%	20%
Average service disruption rate	49%	11.9%	95.8%	16.7%

D. Reconfiguration Time Points Scheduling

Dynamic bandwidth allocation techniques reconfigure the network in relation to traffic demand variations. We considered a tidal traffic matrix, with per hour variations. Thus, the maximum resource allocation efficiency η defined by equation (3), is met by scheduling hourly reconfigurations $\mathcal{T} = \{1, 2, ..24\}$.

$$\eta = \frac{\text{Total\_Demanded\_Bandwidth}}{\text{Total\_Allocated\_Bandwidth}} \tag{3}$$

However, hourly reconfigurations are not well accepted by service operators. A solution is to reduce the reconfiguration time points ($|\mathcal{T}| < 24$) by scheduling reconfiguration events into specific time points $t \in \mathcal{T}$, creating a trade-off: a decrease of the reconfiguration time points $|\mathcal{T}|$ produce an increase of bandwidth over-provisioning (in consequence, increasing power consumption).

Given the traffic matrix of an specific day and lower threshold of the bandwidth allocation efficiency (expected efficiency $\bar{\eta}$), Algorithm 4 describes a *Simulated Annealing*-based heuristic method for optimizing the reconfiguration scheduling ($\mathcal{T}$) by finding the minimum number of reconfiguration time points ($|\mathcal{T}|$) that meet the expected allocation efficiency ($\eta \geq \bar{\eta}$).

E. Complexity Analysis

In the worst case, Algorithm 2 performs bandwidth allocation for each hour of the day ($|\mathcal{T}| = 24$). The complexity of Algorithm 2 is broken into two components: off-line and on-line phases.

Phase 1 – Off-line Planning Optimization: in Section IV-D we gave an idea of VWP and WP problems complexity. This models must be solved at each hour of the day $|\mathcal{T}| = 24$ using the predictable traffic demand patterns ($h_{d,t}$).

Phase 2 – On-line heuristic routing: At each reconfiguration time point, and for each demand the on-line component of the Algorithm 2 must perform: short-time traffic prediction, optimal weights computation and link-disjoint path-pair computation. The worst case complexity of the heuristic is dominated by the calculation of the optimal weights: 1) VWP: grows with $O(V^2(V-1)^2RE)$ 2) WP: growth with $O(V^2(V-1)^2REWF)$, where W and F are the maximum number of wavelengths channels and fibers, respectively.

VI. RESULTS

A. Power Consumption Models

In this work we only considered the power consumption of optical layer. Power data of components are based on the models

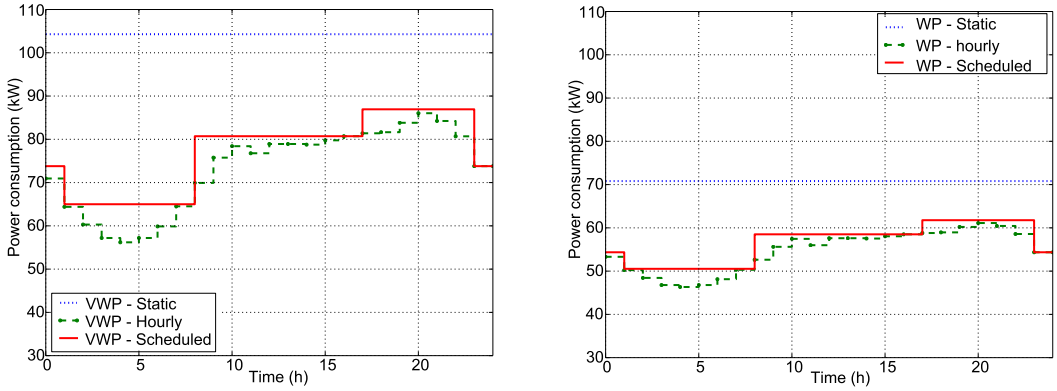

Fig. 5. Optical layer power consumption of the mobile metro-core network under predictable aggregated traffic using three of-line resource allocation methods: Static, Hourly and Scheduled (Time point optimized) for VWP (left) and WP (right) models.

given in [20], that were used to set the weights in the objective functions of equations (1) for VWP and (2) for WP.[6]

The optical layer power dissipation of VWP (full wavelength conversion scenario) can be obtained by (4), where V is the number of OXCs (one per CN) in the network, with a fix consumption of $\psi = 150$ W per OXC. For a line-rate of $L = 10$ Gbit/s, the power dissipation of transponder/muxponder per active wavelength (in one direction) is $\beta = 25$ W. The cost per active fiber (f_e) in the OXCs is $\gamma = 85$ W (optical switching), and $\zeta = 50$ W (add/drop ports). A WDM terminal consumes $\mu = 120$ W (two terminals are installed per fiber). The optical line amplifier (OLA) dissipates $\alpha = 32.5$ W per active fiber.

$$P^{VWP} = \psi V + \beta \sum_{e \in \mathcal{E}} w_e + (\alpha + \mu + \gamma + \zeta) \sum_{e \in \mathcal{E}} f_e \quad [W] \tag{4}$$

The power dissipation of WP (optical bypass scenario) is given by (5). In WP each connection request is satisfied by two lightpaths, therefore the contribution of β W and ζ W are independent of the routing. Accordingly, the only routing dependent variable that affects the power consumption is f_e, with a cost of $\alpha + \mu + \gamma$ W.

$$P^{WP} = \psi V + (\beta + \zeta) \sum_{d \in D} r_d + (\alpha + \mu + \gamma) \sum_{e \in \mathcal{E}} f_e \quad [W] \tag{5}$$

B. Off-line Numerical results

Figs. 5(a) and 5(b) depicts the results of total power consumed (kW) for three different approaches of VWP and WP models, respectively. The flat doted lines represent the static network configuration, where all the elements are active to cope with the peak hour demand of the historical data set. The step-like dashed curves with changes every hour, correspond to minimization of active resources, by solving one instance of the optimization models per hour ($|\mathcal{T}| = 24$). The continuous curves with long steps represent the behavior of a network that schedules a reduced set of reconfigurations per day ($|\mathcal{T}| < 24$), using the heuristic method presented in subSection V-D. At least 20% of energy dissipation E (kWh) per day can be saved using dynamic network operation in both WP and VWP cases.

Our results demonstrate that WP (reducing OEO conversions with optical bypass) is more energy efficient than VWP for mobile metro-core networks. WP consumes 22% less energy E than VWP. However, table III shows that WP is more prone to service disruption than VWP. We considered that service disruption in VWP is experienced only for changes in the routing assignment (RA) of each request, while in the WP, due to wavelength continuity constraint, wavelength reassignments must also be taken into account, reflecting a great increase of the disruption rate defined by equation (6).

[6]Symbols $\mathcal{E}, e, w_e, f_e, \mathcal{D}, d, r_d$, were defined in Sections IV and V.

TABLE IV
ON-LINE RESULTS – AVERAGE ENERGY CONSUMPTION INCREASE

	On-Line Matheuristic	On-line Heuristic (Fixed weight)
VWP	1.5%	8.9%
WP	1.3%	9.7%

$$\text{Average Disruption rate} = \frac{\text{Total\_disrupted\_requests}}{\text{Total\_requests}} \tag{6}$$

Table III summarizes the trade-off between energy dissipation E kWh, and service disruption when using dynamic resource allocation. Our results prove that by properly scheduling the reconfigurations time points it is possible to considerably reduce service disruption rate (WP from 95.8% to 16.7% and VWP from 49% to 11.9%), with a small penalty on energy savings (WP from 23% to 20% and VWP from 29.7% to 26%).

The common approach in today's mobile metro-core networks is similar to the static VWP scenario ($E =$ 2502.9 [kWh per day]), so it is possible to save up to 47.5% of energy per day using the proposed load adaptive operation with optical bypass WP ($E = 1314$ [kWh per day]).

C. On-line results

In order to assess the performance of the proposed matheuristic, a Discrete event simulator (DES) was built using SimPy, a process-based DES framework based on Python. The on-line procedures were tested over one month of real-time metropolitan tidal traffic.

Figs. 6(a) and 6(b) provide a comparison of the proposed on-line matheuristic (described by Algorithm 2) with the off-line optimization, and simple on-line heuristic (based on minimum cost algorithm using number of hops as link weights) for VWP and WP, respectively. Table IV, summarizes the percentage of daily energy dissipation savings when using: off-line

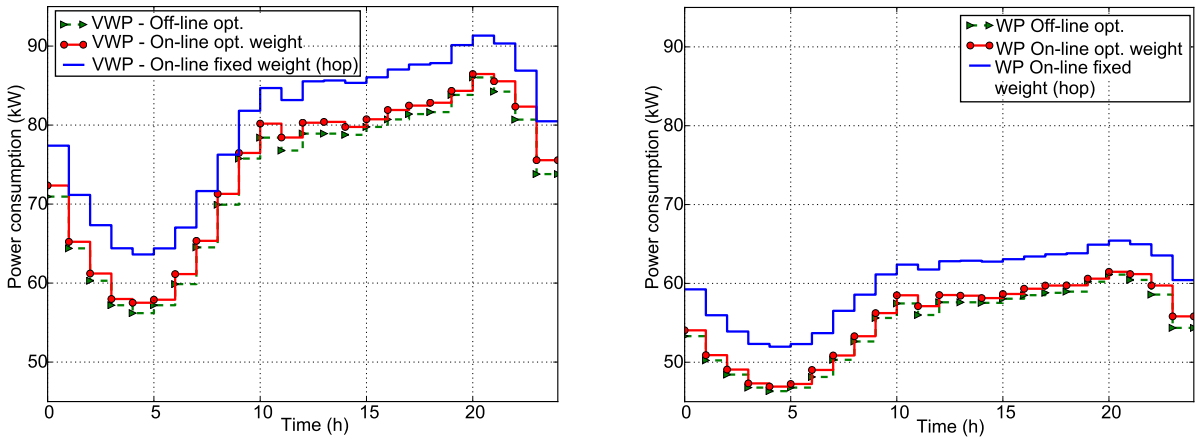

Fig. 6. Energy dissipation in the mobile metro-core network for three different methods: off-line Optimization (under predictable aggregated traffic), on-line matheuristic and on-line heuristic (average value over one month of real-time traffic), using VWP (left) and WP (right).

optimization, matheuristic and heuristic methods. The results demonstrate the effectiveness of the proposed matheuristic, with an optimality gap below 1.5% in the average energy dissipation, while the simple heuristic displays an optimality gap of almost 10%.

VII. Conclusions

In this paper, we analyzed the use of aggregated tidal traffic patterns for energy efficient dynamic optical routing in mobile metro-core networks. Using a real dataset from a Chinese city, we showed that the highly predictability spatio-temporal patterns in the aggregated traffic of the metro-core give a valuable information to optimize the network resource allocation. By knowing the predictable traffic demands, we proposed two off-line optimization models for dynamic resource allocation and reported daily energy savings of more than 20% while effectively responding to traffic load variations.

The smaller energy dissipation was achieved by the dynamic WP model (Section IV-C) with savings up to 47.5% when compare with static VWP, showing the advantages of load adaptive network operation and optical bypass, that thanks to the small link length of a mobile metro-core network can completely avoid optical regeneration. The on-line approach manage unpredictable traffic components alongside with the predictable components, with a small optimality gap. The scheduling procedure is an interesting trade-off between energy efficiency and service disruption. It allows to optimize the reconfiguration time points, in order to reduce disruption while keeping energy efficiency over an specified threshold.

This is an initial study for green mobile metro-core networks. We are now developing a more sophisticated VWP model that includes both traffic grooming and optical bypass based on traffic conditions, and traffic pattern identification.

References

[1] Ericson, "Ericson mobiliy report," 2016. [Online]. Available: http://www.ericsson.com

[2] Cisco Visual Networking Index, "Global mobile data traffic forecast update, 2015-2020," 2016. [Online]. Available: http://www.cisco.com/

[3] Mobile and wireless communications Enablers for the Twenty-twenty Information Society (METIS), "Channel Models," ICT-317669-METIS/D1.4, 2015.

[4] C. Song *et al.*, "Limits of predictability in human mobility," *Science*, vol. 327, no. 5968, pp. 1018–1021, 2010.

[5] Z. Niu, "Tango: Traffic-aware network planning and green operation," *IEEE Wireless Commun.*, vol. 18, no. 5, pp. 25–29, Oct. 2011.

[6] R. Alvizu *et al.*, "Energy aware optimization of mobile metro-core network under predictable aggregated traffic patterns," in *Proc. IEEE Int. Conf. Commun.*, May 2016, pp. 1–7.

[7] M. Afanasyev *et al.*, "Analysis of a mixed-use urban wifi network: When metropolitan becomes neapolitan," in *Proc. ACM SIGCOMM Conf. Internet Meas.*, 2008, pp. 85–98.

[8] C. Lange and A. Gladisch, "Energy efficiency limits of load adaptive networks," in *Proc. Opt. Fiber Commun. Conf.*, 2010, pp. 1–3.

[9] C. Peng *et al.*, "Traffic-driven power saving in operational 3G cellular networks," in *Proc. Int. Conf. Mobile Comput. Netw.*, 2011, pp. 121–132.

[10] L. Budzisz *et al.*, "Dynamic resource provisioning for energy efficiency in wireless access networks: A survey and an outlook," *IEEE Commun. Surveys Tut.*, vol. 16, no. 4, pp. 2259–2285, Oct.–Dec. 2014.

[11] R. Wang *et al.*, "Energy saving via dynamic wavelength sharing in TWDM-PON," *IEEE J. Sel. Areas Commun.*, vol. 32, no. 8, pp. 1566–1574, Aug. 2014.

[12] Z. Zhong *et al.*, "Considerations of effective tidal traffic dispatching in software-defined metro IP over optical networks," in *Proc. Opto-Electron. Commun. Conf.*, Jun. 2015, pp. 1–3.

[13] Z. Zhong *et al.*, "Energy efficiency and blocking reduction for tidal traffic via stateful grooming in IP-over-optical networks," *J. Opt. Commun. Netw.*, vol. 8, no. 3, pp. 175–189, Mar. 2016.

[14] M. Howard, "Using carrier ethernet to backhaul LTE," Infonetics White Paper, 2011.

[15] R. Nadiv and N. Tzvika, "Wireless backhaul topologies: Analyzing backhaul topology strategies," Ceragon White Paper, 2010.

[16] B. Mukherjee, *Optical WDM Networks*. New York, NY, USA: Springer-Verlag, 2006.

[17] M. Tornatore, G. Maier, and A. Pattavina, "Capacity versus availability trade-offs for availability-based routing," *J. Opt. Netw.*, vol. 5, no. 11, pp. 858–869, Nov. 2006.

[18] J. Yuan, Y. Zheng, and X. Xie, "Discovering regions of different functions in a city using human mobility and POIs," in *Proc. 18th ACM SIGKDD Int. Conf. Knowl. Discovery Data Mining*, 2012, pp. 186–194.

[19] Y. Xu *et al.*, "Affinity-based human mobility pattern for improved region function discovering," *J. China Universities Posts Telecommun.*, vol. 23, no. 1, pp. 60–67, 2015.

[20] W. Van Heddeghem *et al.*, "Power consumption modeling in optical multilayer networks," *Photon. Netw. Commun.*, vol. 24, no. 2, pp. 86–102, 2012.

[21] M. Lippi, M. Bertini, and P. Frasconi, "Short-term traffic flow forecasting: An experimental comparison of time-series analysis and supervised learning," *IEEE Trans. Intell. Transp. Syst.*, vol. 14, no. 2, pp. 871–882, Jun. 2013.

[22] C. Chen and S. Banerjee, "A new model for optimal routing and wavelength assignment in wavelength division multiplexed optical networks," in *Proc. IEEE 15th Annu. Joint Conf. Comput. Soc.*, Mar. 1996, vol. 1, pp. 164–171.

[23] R. Bhandari, *Survivable Networks: Algorithms for Diverse Routing*. Norwell, MA, USA: Kluwer, 1998.

Authors' biographies not available at the time of publication.